HOKKAIDO UNIVERSITY

Title	Study of Deuterium Isotope Separation by PEFC
Author(s)	Shibuya, Shota; Matsushima, Hisayoshi; Ueda, Mikito
Citation	Journal of the electrochemical society, 163(7), F704-F707 https://doi.org/10.1149/2.1321607jes
Issue Date	2016-07-20
Doc URL	https://hdl.handle.net/2115/62424
Rights	© The Electrochemical Society, Inc. 2016. All rights reserved. Except as provided under U.S. copyright law, this work may not be reproduced, resold, distributed, or modified without the express permission of The Electrochemical Society (ECS). The archival version of this work was published in Journal of the electrochemical society, volume 163, Issue 7, pp. F704-F707, 2016.
Type	journal article
File Information	Manuscript-ECS-revise.pdf

Hokkaido University Collection of Scholarly and Academic Papers : HUSCAP

Study of Deuterium Isotope Separation by PEFC

Shota Shibuya, Hisayoshi Matsushima* and Mikito Ueda

[1]*Faculty of Engineering, Hokkaido University,*
Kita 13 Nishi 8, Sapporo, Hokkaido 060-8628, Japan
**Corresponding Author: matsushima@eng.hokudai.ac.jp*
Tel. & Fax +81-11-7066352

ABSTRACT

Hydrogen evolution and oxidation reactions were studied on a polycrystalline platinum electrode in 0.05 M D_2SO_4 solution at 298 K by using a rotating disk electrode, focusing on the kinetic isotope effect on reactivity. The polarization measurements in the evolution reaction regime, on the one hand, revealed two Tafel regions: at low overpotentials close to the equilibrium potential, the Tafel slope was 0.039 V dec^{-1}, suggesting a Volmer-Tafel mechanism; and at potentials around 0.05 V or lower, a slope of 0.168 V dec^{-1} indicated that a transition to a Heyrovsky-Tafel mechanism occurred. In the oxidation reaction regime, on the other hand, a single Tafel slope of 0.055 V dec^{-1} was observed at potentials of 0.08 V or lower. Comparing between the deuterium and protium data for the kinetic factors supported the presence of an isotope effect, whereby the deuterium was more easily dissociated on the platinum electrode. The present kinetic result supported the deuterium separation of polymer electrolyte fuel cell (PEFC) in which the mixture gases of H_2 and D_2 were purged. The deuterium separation factor increased with increasing in the hydrogen utilization. This suggests a new isotope separation technique and also provides useful data for fuel cells.

Keywords: isotope effect; separation factor; deuterium; electrolysis; hydrogen oxide reaction; hydrogen evolution reaction; fuel cell

1. Introduction

Hydrogen isotopes are important for fission and fusion reactors [1]. Deuterium, which comprises 0.0149% of hydrogen, is found in natural water, whereas tritium is artificially produced as a by-product of fission reactors.

Techniques of hydrogen isotope separation include several approaches such as distillation [2], chemical exchange [3], quantum sieving [4], and so on [5-7]. Whiticar reported that the bacterial reduction of hydride is associated with a kinetic isotope effect resulting in the enrichment of deuterium [8]. However, most methods are ineffective and have low separation factors. Large-scale plants must deal with enormous volumes of water for isotope enrichment, and especially a new separation technology for tritium at the Fukushima Daiichi Nuclear Power Plant in Japan is urgently required.

One of the most practical methods is CECE (combined electrolysis catalytic exchange) method [9-13]. This method combines electrolysis with chemical exchange reaction. Hydrogen generated in electrolysis is passed into a column mixed with kogel catalyst and Dixon rings. The isotope exchange reaction occurs at the catalytic site, thereby deuterium or tritium can be enriched. This is one of the practical methods due to the reuse of generated hydrogen and high separation factor. However, the electrolysis consumes a huge amount of electric energy and the catalyst requires a lot of noble metal.

Water electrolysis has long been studied for deuterium separation [14-20]. This method has reported the highest separation factor. For example, separation factors of 5–8 are reported for platinum [21] and the highest values of 10–13 are for iron metal [22]. The separation mechanism is attributed to the slower discharge reaction of deuterons than protons. As well as CECE method, the electrolysis is not suitable for large production of hydrogen isotopes. Therefore, we have been proposing a new electrolytic deuterium separation system using a fuel cell. It is suggested by calculation that the new system remarkably should reduce electric energy consumption for heavy water production by reusing the hydrogen and oxygen gases at a fuel cell [23]. However, the hydrogen isotope effect of a fuel cell is not experimentally investigated very much. Recently Oi *et al*. reported that the hydrogen isotope could occur at a fuel cell [24, 25]. The deuterium separation factor was simulated to be from 3.5 to 4.0 depending on the hydrogen utilization.

The kinetics of the hydrogen evolution reaction (HER) is still an important

topic in electrochemistry for both practical applications and fundamental studies. Thus, there are many studies of the kinetic factors for polycrystalline platinum electrodes [26-28]. However, there are a few experimental studies on the kinetic factors of the deuterium evolution reaction (DER) [29]. Previously, Bockris et al. reported that the Tafel slope of DER was 0.026 V dec^{-1}, which was similar to that of HER (0.029 V dec^{-1}), whereas the exchange current of DER was much smaller than that of HER [30].

The hydrogen oxidation reaction (HOR), which is the reverse reaction of HER and the main reaction in a fuel cell, remains the subject of ongoing investigation [31-34]. Moreover, the fundamental kinetic data of the deuterium oxidation reaction (DOR) have not been measured. In this study, we investigate the isotope effect in the hydrogen electrode reaction on a platinum electrode under high-concentration deuterium conditions and then demonstrate the deuterium separation by using PEFC.

2. Experimental

2.1 Measurement of hydrogen electrode reactions

The measurements were conducted under a pure hydrogen or deuterium gas atmosphere. The working electrode was a 0.785 cm^2 polycrystalline platinum disk (Pt 99.99%, Nilaco Corp.) and the counter electrode was a coiled platinum wire. The electrodes were cleaned by ultrasonication in acetone for 30 min and washing in distilled water. They were annealed for 5 min under hydrogen atmosphere and quenched in distilled water in order to activate the surface. The reference electrode was Hg/Hg_2SO_4 saturated with potassium sulfate. A rotating disk electrode (Model 636, EG & G) was used with rotation rates of 900, 1600, 2500, and 3600 rpm [35, 36]. The polarization curves were recorded under potential control by a potentiostat (Model SP-50, Biologic). A sulfuric acid solution of 0.05 M (98 wt% H_2SO_4, Wako Pure Chemical Ind.) was adjusted with distilled water for the protium experiment. A deuterated sulfuric acid solution of 0.05 M (98 wt% D_2SO_4, Sigma-Aldrich) was made with heavy water (99.9 at% D_2O, Isotech) for the deuterium experiment. Pure hydrogen or deuterium gas was bubbled through the electrolyte for 2 h. The solution temperature was maintained at 298 K.

2.2 Measurement of the separation factor at PEFC

JARI standard cell (FC Development Corp.) was employed as PEFC. A

membrane electrode assembly (50 × 50 mm) was composed of Nafion electrolyte (NRE-212) and two catalytic layers loaded with platinum catalyst (Pt 0.52 mg cm^{-2}). PEFC was operated at 298 K and the power generation was controlled under constant current mode (0.0 A - 1.2 A) adjusted by a variable resistor unit (Kikusui Electronics Corp., PLZ 164WA).

Deuterium separation factor, α, of PEFC was measured by quadrupole mass spectrometer (QMS) (Ulvac Corp., Qulee-HGM 202). Figure 1 shows the schematic experimental setup for obtaining α at PEFC. The humidified O_2 gas of 50 mL min^{-1} was supplied into cathode. The mixture gases of H_2 and D_2 were used at anode. The mixing ratio was adjusted by mass flow controller (Alicat Corp., MC-200SCCM-D). The flow rate of H_2 and D_2 was 20 mL min^{-1} and 2 mL min^{-1}, respectively. QMS monitored the gas component exhausting from anode before and after PEFC operation. It recorded the ion current of mass number (m = 2, 3 and 4) for 8 hours at which the ion current reached steady state value.

3. Results and Discussion

3.1 Kinetics of Hydrogen Electrode Reactions

The fundamental experiment of hydrogen electrode reaction was conducted by using rotating disk electrode under a flow of hydrogen or deuterium gas to exclude oxygen. Before the electrochemical measurements, the open circuit potential (OCP) was recorded as -0.725 V in H_2SO_4 and -0.730 V in D_2SO_4 electrolyte. The small potential difference of 0.005 V is explained by the Gibbs free energy of deuterium corresponding to -0.013 V at 298 K [29].

The polarization curves were measured by linear sweep voltammetry at a scan rate of ±0.01 V s^{-1}. Figure 2 shows the current density for HER/HOR and DER/DOR for a scanning range of ±0.3 V from OCP. The reduction reaction currents were independent of the rotation rate in both electrolytes, whereas the oxidation currents were significantly affected by forced convection at more than -0.65 and -0.70 V HER/HOR and DER/DOR, respectively. The limiting current densities, which were induced by the diffusional limitation of the dissolved hydrogen gas, appeared at high electrode potentials (E > -0.5 V).

3.1.1 HER and DER

The Tafel slopes for HER and DER were determined at low overpotentials (0 V ≥ η ≥ -0.15 V), as seen in Fig. 3. Two Tafel slopes were observed for HER in H_2SO_4 solution. The slope changed around η = -0.05 V. The value was 0.034 V dec^{-1} at low overpotentials and 0.143 V dec^{-1} at high overpotentials. The mechanism of HER on polycrystalline platinum has been thoroughly investigated [34-37]. The low slope value corresponds to the Volmer-Tafel mechanism and the high slope value corresponds to the Heyrovsky-Tafel mechanism. The Tafel slopes of DER, too, could be divided into two Tafel regions. The slope value was 0.039 V dec^{-1} at low overpotentials (η ≥ -0.05 V) and 0.168 V dec^{-1} at high overpotentials. The slope values of HER and DER under Volmer-Tafel conditions were similar, whereas the difference between the slopes increased under the Heyrovsky-Tafel regime in this work.

The Tafel slopes were extrapolated to the *x*-axis to obtain the exchange current density. The values for HER, $i_{0(H+)}$, and DER, $i_{0(D+)}$, were 0.031 and 0.018 mA cm^{-2}, respectively. The ratio of $i_{0(H+)}/i_{0(D+)}$ was 1.72, which was in good agreement with other result [30]. The present values of the exchange current density are larger than general values [28-30]. This might be explained by surface roughness. Thus, we simply calculated the surface area as the geometry area.

3.1.2 HOR and DOR

The anodic currents did not depend on the rotational rate at η ≤ 0.08 V, which suggests that the oxidation reactions of hydrogen or deuterium were kinetically controlled. As the anodic potential increased, the reactions were under a mixture of kinetic and diffusion control. To clarify the Tafel region, the current density was corrected by the limiting current [34]. Fig. 4 shows Tafel plots of mass transfer-corrected currents for the HOR and DOR at low anodic overpotentials.

There was one Tafel region at low overpotentials (η ≤ 0.08 V) for HOR and DOR in contrast to HER. The Tafel region of HOR began at η ≈ 0.04 V. The slope value of HOR was 0.091 V dec^{-1}, which was much larger than that of the Volmer-Tafel mechanism. This might be explained by the slow dissociation of hydrogen gas molecules, although more detailed studies are required to confirm this. The Tafel slope of DOR was observed from a lower overpotential (η ≥ 0.03 V). The slope value was 0.055 V dec^{-1}, which was significantly smaller than that of HOR. Although the exchange current densities in Fig. 4 did not match those in Fig. 3, the ratio of $i_{0(H2)}/i_{0(D2)}$

was 0.46.

Comparison between the deuterium and protium data for the kinetic factors indicated an isotope effect: deuterium was more easily dissociated on a platinum electrode, suggesting the deuterium separation at a fuel cell. Therefore, we demonstrated the deuterium separation by using PEFC at the next section.

3.2 Deuterium Separation by PEFC

The mixture gases was directly connected to QMS (gas line I in Fig. 1). The ratio of H and D was checked. The results of QMS showed that the gas composition was very stable during the measurement. As seen in Fig. 5 (a), the ion current of mass number $m = 4$ was about 1/10 times less than that of $m = 2$.

Once the mixture gas was introduced to anode at PEFC (gas line II in Fig. 2), the ratio of $m = 3$ was significantly increased instead of decreasing in that of $m = 4$ (Fig. 5 (b)). This reversal phenomenon of ion current between $m = 3$ and $m = 4$ was unrelated to the power generation. Taking into account of the unchanged atomic ratio of H and D might give us one explanation. When the both gases of H_2 and D_2 are passed to the catalytic layer, HD gas ($m = 3$) is generated by isotope exchange reaction as expressed in Eq. (1).

$$H_2 + D_2 \rightarrow 2HD \quad (1)$$

The exchange reaction is reported to occur on platinum surface [38, 39]. The almost all molecules of H_2 and D_2 introduced into PEFC were converted to HD since the ion current of $m = 4$ was remarkably dropped. The gas diffusion layer and nano-sized Pt catalyst, which are researched and developed for PEFC, might contribute to the high activity for Eq. (1).

The ratio of gas components changed after PEFC was operated at 1.2 A (output voltage = 0.78 V) as seen in Fig. 5 (b). The ion current of HD and D_2 decreased while H_2 one slightly increased. It took 1.5 hours to reach steady state. The transient time might be attributed to the replacement of QMS chamber by the reacted gases. The gases containing deuterium was preferentially consumed at PEFC. It was found that the composition ratio of D_2 decreased larger than that of HD. This coincided with the kinetic isotope effect of which the degree is enlarged with increasing in mass number

[40].

The deuterium separation factor was obtained by measuring the outlet gas (gas lines II in Fig. 1) from PEFC. The factor was calculated by the following equation,

$$\alpha = ([H]/[D])_a / ([H]/[D])_b \quad (2)$$

where [H] and [D] are atomic fractions of protium and deuterium, the subscript (a) and (b) refers to *after* and *before* starting the power generation.

The separation factor was calculated at 5 hours after starting PEFC. Figure 6 shows α depending on the output current. The factor value increased from α = 1.1 at 0.05 A to α = 4.6 at 1.2 A. The isotope condensation toward the produced water was accelerated with increasing in the output current. This is probably attributed to the hydrogen utilization. Thus, low fuel utility rises the unreacted mixture gases which can pass only through the gas diffusion layer. Although the factor of 4.6 is higher than other deuterium separation methods such as CECE, the good separation performance is expectedly achieved by developing catalyst and operation conditions, since the present fuel utilization of 40 % was still low.

4. Conclusions

In order to investigate possibility of the hydrogen isotope separation by PEFC, the kinetic electrochemical factors were investigated and the deuterium separation was demonstrated practically.

The exchange current density and Tafel slope measured by a rotating disk electrodes indicated the isotope effect on the hydrogen oxidation reaction as well as on the evolution reaction. The values of exchange current density and Tafel slope in HOR were 0.130 mA cm^{-2} and 0.091 V dec^{-1}, while the values in DOR were 0.057 mA cm^{-2} and 0.055 V dec^{-1}, respectively.

PEFC with Nafion MEA was galvanostatically operated under introducing the mixture gases of H_2 and D_2. The deuterium separation factor significantly increased with increasing in the output current. The maximum value was 4.6 at 1.2 A (0.93 W at 298 K) at the present experiment. Corresponding to the kinetic results, the deuterium could be separated as the produced water through the oxidation reaction. Compared with other separation processes, the large value of α might be attributed to the mixture

effects of the electrochemical reactions and membrane. It will be clarified by investigating the isotope ratio of the produced water the in the future.

ACKNOWLEDGMENT

The authors appreciate financial support from the Ministry of Education, Culture, Sports, Science and Technology (Project No. 26870234). One of the authors, H. Matsushima, wishes to express his sincere gratitude to Inamori Foundation in Japan.

REFERENCE

1. S. J. Zinkle, L. L. Snead, *Ann. Rev. Mater. Res.*, **44**, 241 (2014).
2. Y. Iwai, H. Yoshida, T. Yamanishi, S. Senrui, M. Nishi, *Fusion Eng. Des.*, **49**, 847 (2000).
3. F. Huang, C. G. Meng, *Int. J. Hydrog. Energy*, **35**, 6108 (2010)
4. S. A. FitzGerald, C. J. Pierce, J. L. C. Rowsell, E. D. Bloch, J. A. Mason, *J. Am. Chem. Soc.*, **135**, 9458 (2013).
5. Y. Sakharovski, V. Tkachenko, *J. Radioanal. Nucl. Chem*., **304**, 357 (2015).
6. M. Hankel, Y. Jiao, A. Du, S. K. Gray, S. C. Smith, *J. Phys. Chem.*, **116**, 6672 (2012).
7. K. Watanabe, M. Matsuyama, T. Kobayashi, S. Taguchi, *J. Alloy Com.*, **257**, 278 (1997).
8. M. J. Whiticar, *Chem. Geol.*, **161**, 291 (1999).
9. I. A. Alekseev, S. D. Bondarenko, O. A. Fedorchenko et al., *Fusion Sci. Technol.*, **60**, 1117 (2011)
10. Y. Sun, H. Y. Wang, G. Sang, *Fusion Eng. Des.*, 83, 1400 (2008).
11. T. Sugiyama, Y. Asakura, T. Uda, T. Shiozaki, Y. Enokida, I. Yamamoto, *Fusion Eng. Des.*, 81, 833 (2006).
12. J. M. Miller, S. L. Celovsky, A. E. Everatt, W. R. C. Graham, J. R. R. Tremblay, , *Fusion Sci. Technol.*, **41**, 1077 (2002).
13. H. K. Rae, *Trans. ANS*, **23**, 65 (1976).
14. S. S. Mijanic, A. D. Maksic, N. I. Potkonjak, M. P. M. Kaninski, *Electrochem. Commun.*, **9**, 2179 (2007).
15. B. Dandapan, M. Fleischm, *J. Electroanal. Chem.*, **39**, 315(2002).
16. L. I. Krishtalik, *Electrochim. Acta*, **46**, 2949 (2001).
17. D. L. J. Stojic, S. S. Miljanic, T. D. Grozdic, L. T. Petkovska, M. M. Jaksic, *Int. J. Hydrog. Energy*, **25**, 819 (2000).
18. J. Sperling, H. Tributsch, R. M. F. Streffer, T. A. Redah, C. A. C. Dreismann, *J. Electroanal. Chem.*, **477**, 62 (1999).
19. T. Green, D. Britz, *J. Electroanal. Chem.*, **412**, 59 (1996).
20. B. Topley, H. Eyring, *J. Chem. Physics*, **2**, 17494 (1934).
21. M. Hammerli, J. P. Mislan, W. J. Olmstead, *J. Electrochem. Soc.*, **117**, 751 (1970).
22. H. Matsushima, T. Nohira, Y. Ito, *Electrochim. Acta*, **49**, 4181 (2004).

23. H. Matsushima, T. Nohira, T. Kitabata, Y. Ito, *Energy*, **30**, 2413 (2005).
24. S. Yanase, T. Oi., *Z. Naturforsch*, **70**, 429 (2015).
25. S. Yanase, T. Oi, *J. Nucl. Sci. Technol.*, **50**, 808 (2013).
26. P. M. Quaino, M. R. Chialvo, A. C. Chialvo, *Electrochim. Acta*, **52**, 7396 (2007).
27. M. C. Tavares, S. A. S. Machado, L. H. Mazo, *Electrochim. Acta*, **46**, 4359 (2001).
28. H. Kita, *J. Electrochem. Soc.*, **113**, 1095 (1966).
29. J. D. E. McIntyre, M. Salomon, J. *Phys. Chem.*, **72**, 2431 (1968).
30. J. O'M. Bockris, D. F. A. Koch, *J. Phys. Chem.*, **65**, 1941 (1961).
31. T. Shinagawa, A. T. Garcia-Esparza, K. Takanabe, *ChemElectroChem*, **1**, 1497, (2014).
32. J. Durst, A. Siebel, C. Simon, F. Hasche, J. Herranz, H. A. Gasteiger, *Energy Environ. Sci.*, **7**, 2255 (2014).
33. W. Sheng, H. A. Gasteiger, Y. S. Horn, *J. Electrochem. Soc.*, **157**, B1529 (2010).
34. N. M. Markovic, B. N. Grgur, P. N. Ross, *J. Phys. Chem. B*, **101**, 5404 (1997).
35. B. E. Conway, B. V. Tilak, *Electrochim. Acta*, **47**, 3571 (2002).
36. M. S. Rau, M. R. Gennero de Chialvo, A. C. Chialvo, *J. Power Sources*, **229**, 210 (2013).
37. P. Mandin, T. Pauporte, P. Fanouillere, D. Lincot, *J. Electroanal. Chem.*, **565**, 159 (2004).
38. L. Ye, D. Luo, W. Yang, W. Guo, Q. Xu, C. Jiang, *J. Hydrog. Energy*, **38**, 13596 (2013).
39. B. M. Habersberger, T. P. Lodge, F. S. Bates, *Macromolecules*, **45**, 7778 (2012).
40. W. B. Zhang, I. J. Burgess, *J. Electroanal. Chem.*, **668**, 66 (2012).

Figure Captions

Figure 1

Schematic illustration of experimental setup for measuring the deuterium separation by using PEFC.

1. H_2 gas, 2. D_2 gas, 3. O_2 gas, 4. Mass flow controller; 5. Gas mixture, 6. Electrolyte membrane assembly, 7.Variable resistor; 8; Q-mass.

Figure 2

Polarization curves for (a) HER/HOR in 0.05 M H_2SO_4 and (b) DER/DOR in 0.05 M D_2SO_4 on a platinum disk electrode at several rotation rates, 900 rpm (black line), 1600 rpm (blue line), 2500 rpm (green line), and 3600 rpm (red line). Sweep rate is 0.01 V s^{-1}.

Figure 3

Tafel plots of the reduction current for the HER (dotted line) in 0.05 M H_2SO_4 and the DER (solid line) in 0.05 M D_2SO_4 at low cathodic overpotentials at 298 K. Rotation rate is 1600 rpm.

Figure 4

Tafel plots of mass transfer-corrected currents for the HOR (dotted line) in 0.05 M H_2SO_4 and the DOR (solid line) in 0.05 M D_2SO_4 at low anodic overpotentials at 298 K. Rotation rate is 1600 rpm.

Figure 5

Transient behavior of Q-mass ion current for measuring the mixture hydrogen gases collecting from (a) Line I and (b) Line II through PEFC operated at 1.2 A. (H_2 : 20 mL min^{-1}, D_2 : 2 mL min^{-1})

Figure 6

Dependency of deuterium separation factor on the output current of PEFC operated at 298 K. (H_2 : 20 mL min^{-1}, D_2 : 2 mL min^{-1}, O_2 : 50 mL min^{-1})

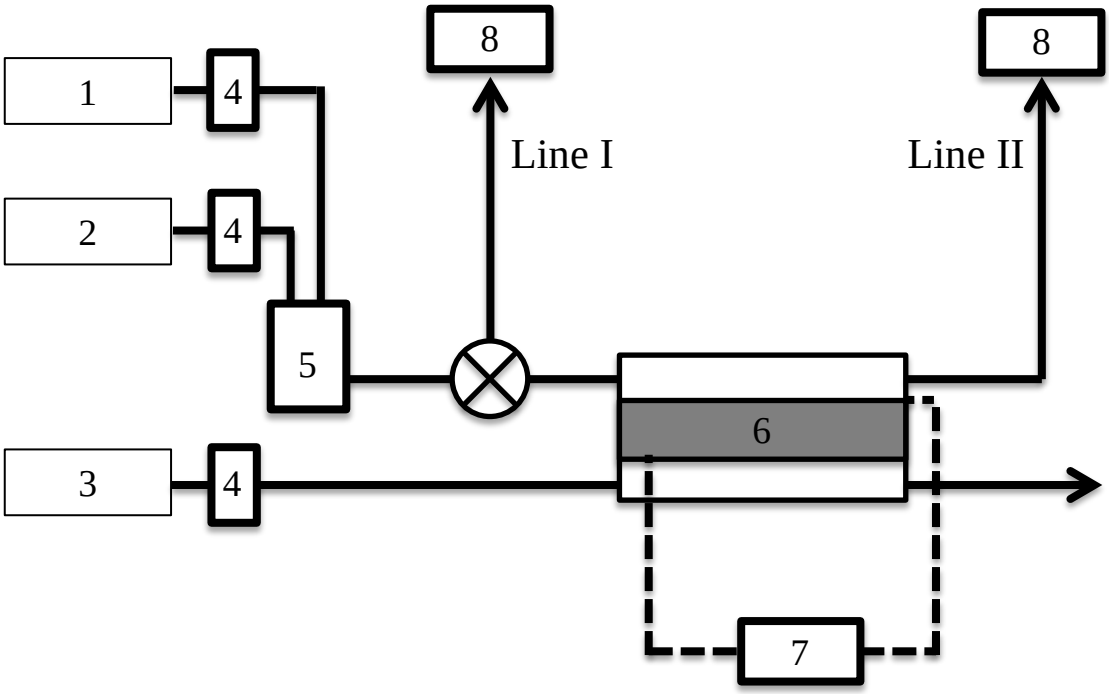

Fig. 1 Schematic illustration of experimental setup for the deuterium separation factor of PEFC.
1. H_2 gas, 2. D_2 gas, 3. O_2 gas, 4. Mass flow controller, 5. Gas mixture unit, 6. Electrolyte membrane assembly, 7.Variable resistor; 8; Q-mass.

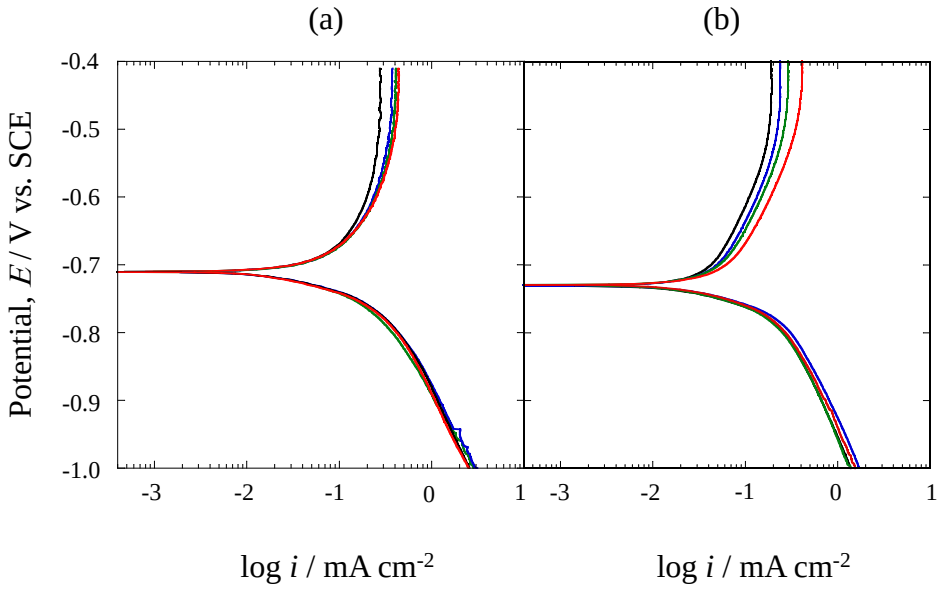

Fig. 2
Polarization curves for (a) HER/HOR in 0.05 M H_2SO_4 and (b) DER/DOR in 0.05 M D_2SO_4 on a platinum disk electrode at several rotation rates, 900 rpm (black line), 1600 rpm (blue line), 2500 rpm (green line), and 3600 rpm (red line). Sweep rate is 0.01 V s^{-1}.

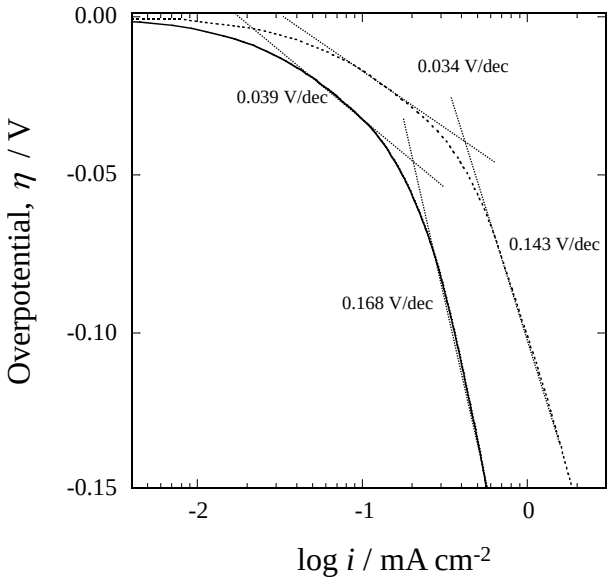

Fig. 3
Tafel plots of the reduction current for the HER (dotted line) in 0.05 M H_2SO_4 and the DER (solid line) in 0.05 M D_2SO_4 at low cathodic overpotentials at 298 K. Rotation rate is 1600 rpm.

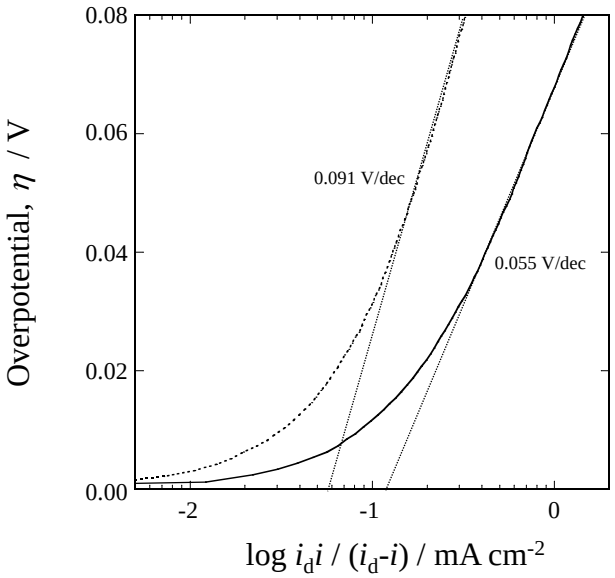

Fig. 4
Tafel plots of mass transfer-corrected currents for the HOR (dotted line) in 0.05 M H_2SO_4 and the DOR (solid line) in 0.05 M D_2SO_4 at low anodic overpotentials at 298 K. Rotation rate is 1600 rpm.

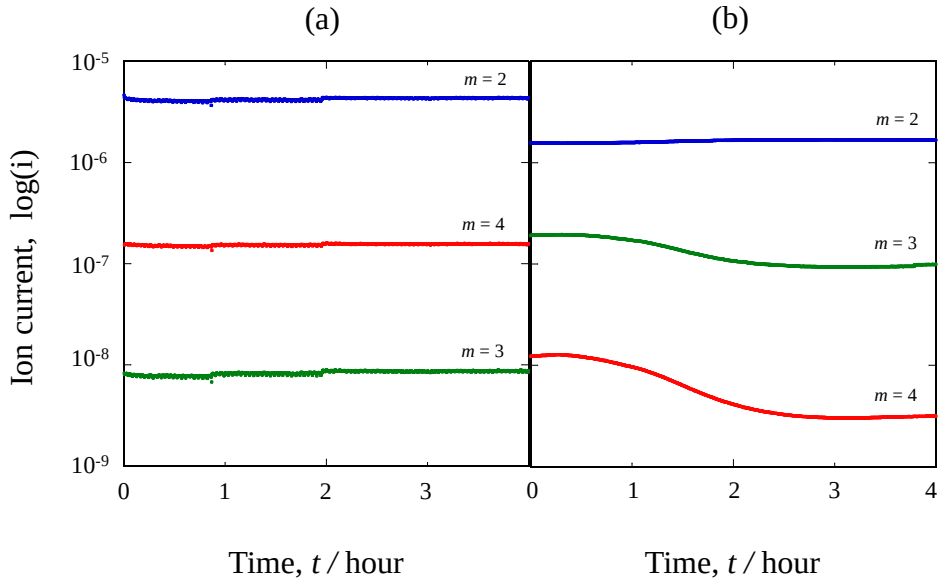

Fig. 5
Transient behavior of Q-mass spectrums for measuring the mixture hydrogen gases collecting from (a) Line I and (b) Line II through PEFC operated at 1.2 A.
(H_2 : 20 mL min^{-1}, D_2 : 2 mL min^{-1})

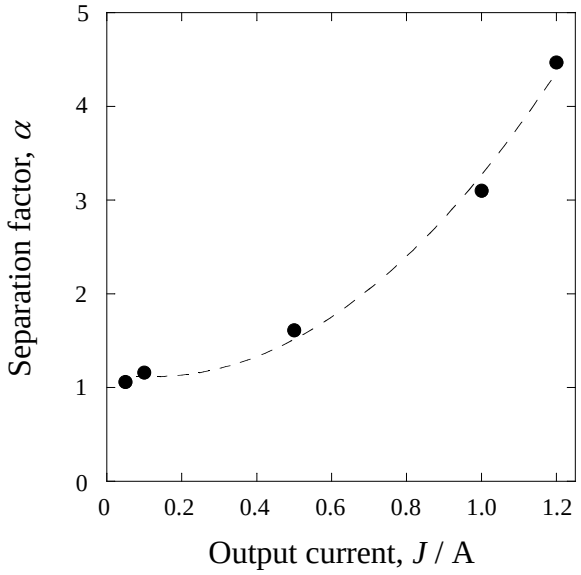

Fig. 6
Dependency of deuterium separation factor on the output current of PEFC operated at 298 K. (H_2 : 20 mL min^{-1}, D_2 : 2 mL min^{-1}, O_2 : 50 mL min^{-1})